

Magnetic properties of diluted band ferromagnet URhAlP. Javorský,^{1,2,*} L. Havela,² F. Wastin,¹ P. Boulet,¹ and J. Rebizant¹¹European Commission, Joint Research Centre, Institute for Transuranium Elements, Postfach 2340, 76125 Karlsruhe, Germany²Department of Electronic Structures, Charles University, Ke Karlovu 5, 121 16 Prague 2, Czech Republic

(Received 14 July 2003; revised manuscript received 20 October 2003; published 18 February 2004)

Crystal structure, magnetization, and specific-heat studies were performed on the $U_{1-x}Th_xRhAl$ and $U_{1-x}Lu_xRhAl$ pseudoternary systems. The parent URhAl compound orders ferromagnetically below $T_C = 27$ K. Dilution of the U sublattice by Th or Lu leads to a rapid decrease of both the magnetic-ordering temperature and the spontaneous magnetic moment. The long-range magnetic order vanishes around 35% Th or 15% Lu substitution. The electronic specific heat shows a maximum in this critical concentration region.

DOI: 10.1103/PhysRevB.69.054412

PACS number(s): 75.30.Cr, 75.40.Cx, 75.50.Cc

I. INTRODUCTION

The $5f$ states in light actinides are generally close to the borderline between localized and itinerant behavior. Their sensitivity to external variables and composition manifests into a large variability of magnetic properties and in some cases even in rather exotic character.¹

The basic features of the development of magnetism in uranium intermetallic compounds are well understood due to variations of the U-U spacing and the strength of the $5f$ -ligand hybridization. Depending on these parameters, magnetic characteristics can develop from the Pauli paramagnetism pertinent to a broad $5f$ -band case to various forms of weak itinerant magnetism up to a local $5f$ moment behavior, which is encountered at a large U-U spacing and a weak hybridization.² The ultimate limit of localized $5f$ states is though found only in singular cases. Several scenarios can be followed when diluting the U sublattice in a U-based intermetallic. In the “local-moment” scenario A, the long-range magnetic order is preserved to a rather low U content and is followed by a glassy state (spin glass or cluster glass) at even higher dilution. The critical concentration of the U ions can be roughly associated with a percolation limit. But in the ultimate case of the dilution limit, the uranium moments are lost in most of cases. Few exceptions of U magnetic moments existing in the dilution limit include the cases of the localized $5f$ states, as U in Au (Ref. 3) or U in $ThRu_2Si_2$.⁴ A different scenario B was observed for U compounds classified as more itinerant. Magnetic ordering as well as magnetic moments decay much faster with the dilution of the U sublattice and the Pauli paramagnetic character is achieved long before the dilution limit.

For the U compounds with the ZrNiAl structure type, which were otherwise studied thoroughly,² only few dilution studies have been performed. One of them, dealing with the (U-Th)CoSn system,⁵ shows the scenario A. UCoSn is a local-moment ferromagnet (although exhibiting itinerant $5f$ states) with $T_C = 80$ K. The ferromagnetism vanishes at around 60% Th.⁵

On the other hand, much stronger hybridization with the Al- p states (due to the smaller size of the Al ions compared to Sn),⁶ yielding a stronger $5f$ itinerancy in UCoAl, leads to the different dilution scenario. In this band metamagnet (the ground state is paramagnetic), the magnetic order can be induced by a small substitution by Y or Lu, resulting in a

typical weak ferromagnet with $\mu_s = 0.20\mu_B/f.u.$ The ferromagnetism disappears rapidly with applied pressure,⁷ and the fact that the Pauli paramagnetic susceptibility was found already for 30% Y (Ref. 8) points to the type-B scenario. Similar fast decay of magnetic ordering was indicated also for an itinerant antiferromagnet UNiAl.^{9,10}

URhAl can be assumed as an intermediate case. Magnetic moment $\mu_s = 0.94\mu_B/f.u.$ [11] does not reach the value of, e.g., UCoSn ($1.2\mu_B/f.u.$) and especially its ordering temperature $T_C = 27$ K is much lower than $T_C = 80$ K in UCoSn. On the other side, both values exceed those of $U_{0.98}Y_{0.02}CoAl$ ($T_C = 14$ K, $\mu_s = 0.10\mu_B/f.u.$).⁷ It is also interesting to compare the development of magnetism in high pressure. For $U_{0.98}Y_{0.02}CoAl$ both T_C and μ_s strongly decrease with hydrostatic pressure p ($dT_C/dp \approx -110$ K/GPa, $d\mu_s/dp \approx -0.8\mu_B/GPa$). For the local-moment systems, T_C follows an initial increasing tendency. The data are not available for UCoSn, but, for example, UPtAl with a presumable similar local-moment behavior exhibits $dT_C/dp = 2.5$ K/GPa, $d\mu_s/dp = -0.027\mu_B/GPa$.¹² For URhAl, T_C has a weakly decreasing tendency ($dT_C/dp = -0.3$ K/GPa).¹³

It is therefore interesting to investigate the dilution behavior of URhAl. In the present work we describe the results of magnetic and thermodynamic studies of the systems (U-Th)RhAl and (U-Lu)RhAl. The two different nonmagnetic elements were chosen to investigate if a size factor plays a role.

II. EXPERIMENT

Polycrystalline samples were prepared by arc melting the stoichiometric amounts of the pure elements under an argon atmosphere. The ingot was melted several times to enhance the homogeneity. Weight loss was checked after melting and found to be negligible. The characterization of the samples was performed by x-ray powder diffraction with a Bruker D8-advance diffractometer, using a monochromated Cu K_α radiation and a position-sensitive detector. Small single crystals isolated from the fragmented button were examined with the Enraf-Nonius CAD4 diffractometer using the monochromated Mo K_α radiation.

The magnetization was studied on powder samples with grains randomly oriented and fixed by an acetone-based glue. Measurements were performed using a superconducting

TABLE I. Atomic positions in LuRhAl.

Atom	x	y	z
Lu	-0.035(2)	0.25	0.178(1)
Rh	0.237(3)	0.25	0.624(2)
Al	0.865(7)	0.25	0.557(6)

quantum interference magnetometer (Quantum Design) in magnetic fields up to 7 T in the temperature range 2–300 K.

The specific heat was measured by the relaxation method using the Quantum Design PPMS-9 system, installed at ITU Karlsruhe in the temperature range 1.8–300 K (down to 0.4 K for samples with 20% and 35% of Th). The samples with a mass of ≈ 10 –20 mg were used for these measurements.

III. RESULTS

A. Crystal structure

The x-ray powder diffraction confirmed the hexagonal ZrNiAl-type structure (space group $P\bar{6}2m$) for the $U_{1-x}Th_xRhAl$ compounds in the whole concentration range.

Unfortunately, the sample with 80% Th contained a larger amount of ThO_2 and other impurity phase, and no thermal treatment led to improved phase purity. Therefore we only determined the lattice parameters of the main phase but did not use this sample for further studies.

In the $U_{1-x}Lu_xRhAl$ series, the hexagonal structure is retained to $x=0.15$. The samples with higher Lu concentration contained already spurious phases. The crystal structure of LuRhAl is orthorhombic TiNiSi-type (space group $Pnma$) with $a=673.2(1)$ pm, $b=412.8(1)$ pm, and $c=787.9(1)$ pm. The refined atomic positions are given in Table I.

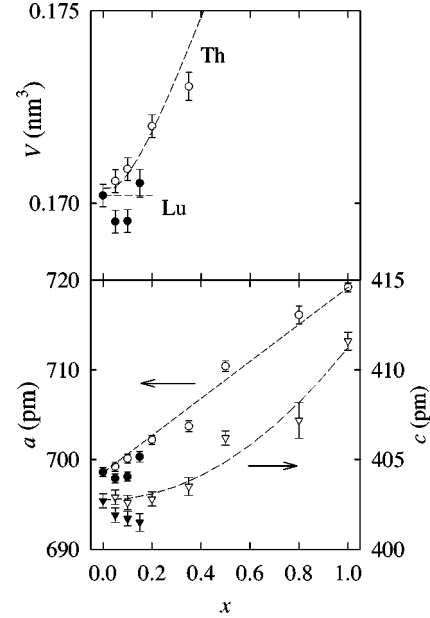


FIG. 1. Concentration dependence of the lattice parameters and the unit-cell volume in $U_{1-x}Th_xRhAl$ (open symbols) and $U_{1-x}Lu_xRhAl$ (filled symbols); lines are guides to the eye.

The lattice parameters of the compounds with the ZrNiAl-type structure are given in Table II and plotted in Fig. 1. The parameter a increases almost linearly with increasing the Th(Lu) concentration. On the other hand, the c parameter seems to stay almost constant for low Th concentration and increases only above $x>0.3$, following roughly a quadratic dependence, and shows a slight decrease for Lu substitution. The internal parameter characterizing the uranium atomic position $x_U=0.580(2)$ remains unchanged for all compounds studied.

 TABLE II. Characteristics of $U_{1-x}Th_xRhAl$ and $U_{1-x}Lu_xRhAl$ materials.

x	a (pm)	c (pm)	T_C (K)	Θ_p (K)	μ_{eff} (μ_B/U)	M (μ_B/U)	M_{6T} (μ_B/U)	γ ($mJ K^{-2} mol f.u.^{-1}$)	S_{mag} ($JK^{-1} mol f.u.^{-1}$) / ($JK^{-1} mol U^{-1}$)	
$U_{1-x}Th_xRhAl$										
0.00	698.6	402.7	27.5(5)	34.5	1.89	0.47(1)	0.54	67(2)	2.32/2.32	
0.05	699.2	402.9	20(1)					93(2)	1.94/2.04	
0.10	700.1	402.6	15(1)	20.8(4)	1.75(1)	0.44(1)	0.50	110(10)	1.64/1.82	
0.20	702.2	402.8	7(2)	5(1)	1.49(1)	0.19(1)	0.30	160(10)	1.10/1.37	
0.35	703.7	403.5		-4.8(5)	1.45(1)		0.22	230(30)		
0.50	710.4	406.2		-22(5)	0.78(3)		0.14	120(20)		
1.00	719.2	411.6						4(1)		
$U_{1-x}Lu_xRhAl$										
0.00	698.6	402.7	27.5(5)	34.5	1.89	0.47(1)	0.54	67(2)	2.32/2.32	
0.05	697.9	401.9	18(1)	22.2(4)	1.45(1)	0.38(1)	0.42	97(5)	1.78/1.87	
0.10	698.1	401.7	13(2)	13.6(5)	1.34(1)	0.23(1)	0.30	135(10)	1.25/1.39	
0.15	700.3	401.5	<1.8	13.6(5)	1.34(1)		0.19	175(30)		
1.00	$Pnma$								3(1)	

^aExtrapolated to 0 T from the Arrott plot at 2 K.

^bDetermined as an extrapolation to 0 K in zero magnetic field.

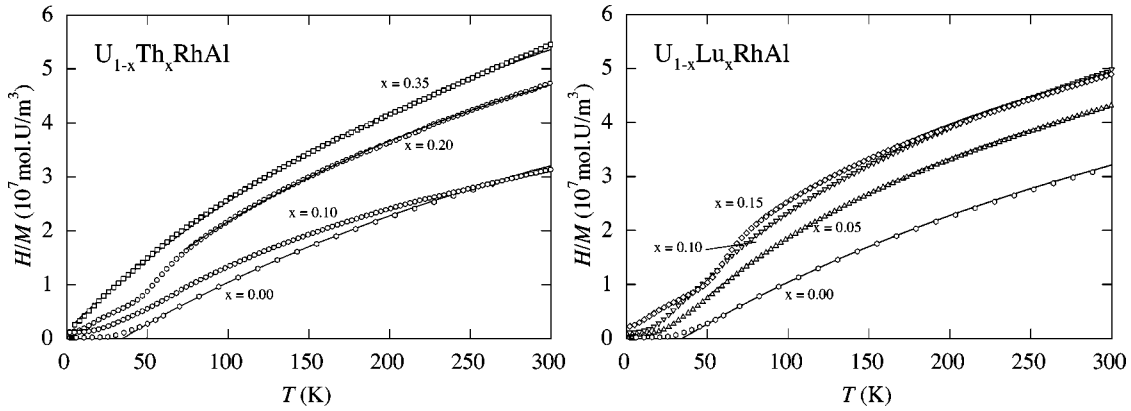


FIG. 2. Temperature dependence of the inverse susceptibility (recalculated per U atom) for $U_{1-x}Th_xRhAl$ and $U_{1-x}Lu_xRhAl$ measured in the field of 4 T. The data for $x=0.10, 0.20$ (Th) and $x=0.10, 0.15$ (Lu) below 70 K are influenced by a small amount of a ferromagnetic impurity and have not been used in the fit.

The uranium sublattice in this crystal structure is characterized by a closer spacing within the basal plane than along the c axis. The shortest U-U distance in URhAl is found within the basal plane, $d_{U-U} = a\sqrt{1-3x_U+3x_U^2} \cong 0.519a$. The U-U spacing perpendicular to the basal plane is equal to the parameter c , that is, as a rule, larger. Introducing larger thorium atoms leads to an expansion of the lattice. First, for low Th concentrations, the a parameter increases being predominantly affected by the bonds in the uranium sublattice within the basal plane. Consequently, the c/a ratio decreases slightly when increasing Th(Lu) concentration. Nevertheless, the c parameter remains considerably larger than the d_{U-U} spacing within the basal plane in the whole concentration range. For the dilution of the U sublattice by smaller Lu atoms, this large increase of the lattice parameter a was not observed.

B. Magnetic measurements

The temperature dependence of magnetic susceptibility in the paramagnetic region follows for all the compounds, except for ThRhAl and LuRhAl displaying a temperature-independent susceptibility ($\chi \approx 5 \times 10^{-10} \text{ m}^3 \text{ mol}^{-1}$), the modified Curie-Weiss (MCW) law (see Fig. 2)

$$\chi = \frac{N_A \mu_0 \mu_B^2 \mu_{eff}^2}{3k_B(T - \Theta_p)} + \chi_0. \quad (1)$$

The values of the effective moment μ_{eff} and the paramagnetic Curie temperature Θ_p in the studied compounds as obtained from our fit to experimental data are given in Table II. The temperature independent term χ_0 is of the order of $1 \times 10^{-8} \text{ m}^3 \text{ mol}^{-1}$ for all the samples. The other symbols in Eq. (1) have their usual meaning. The positive paramagnetic Curie temperature is in agreement with expected ferromagnetic interactions in the magnetically ordered compounds. Performing an analysis on the basis of the MCW law, one has to have in mind two different sources of the temperature-independent term χ_0 . One is the real Pauli susceptibility due to the electrons at the Fermi level. One has to assume that weakly correlated electrons, i.e., those not involved in the

formation of local moments, contribute to this term, and it has to become significant in the high-dilution limit. On the other hand, a bending of $1/\chi(T)$ dependence, which can be very well approximated by adding the χ_0 term to the standard Curie-Weiss expression, appears when measuring susceptibility of a strongly anisotropic polycrystalline material. In such case markedly different Θ_p values exist if the field is applied along different crystallographic directions, and the bending appears due to the averaging over possible orientations of crystallites in the powder sample. This bending is more pronounced in magnetically uniaxial material (easy-magnetization direction, that is, the case of URhAl with the easy-magnetization c axis) than in the case of an easy-plane anisotropy. In the case of this anisotropy, the μ_{eff} values obtained by fitting to the MCW law are smaller than the intrinsic effective moments. Both types of the bending can coexist in the diluted URhAl system, and cannot be distinguished without studies on single crystals. The data obtained from the MCW fit thus merely illustrate tendencies of variations of the paramagnetic susceptibility and need not to be taken as quantitative information on the microscopic parameters. Nevertheless, the reduction of μ_{eff} with proceeding dilution can be concluded unambiguously.

At low temperatures, the susceptibilities for compounds with low Th(Lu) content (see Fig. 3) exhibit a ferromagnetic behavior characterized by a steep increase with an inflexion point in the critical temperature region followed by a slower increase below T_c and tendency to saturation in the $T \rightarrow 0$ K limit. The magnetization curves (see Fig. 4) and the Arrott plots (see Fig. 5) of compounds with low Th(Lu) concentration show also a shape typical for the ferromagnetic ordering. We should mention here that in our case of the randomly oriented powder and the uniaxial magnetocrystalline anisotropy, the values of the magnetic moments determined from our data are 1/2 of the real moments.

The critical temperatures determined from the magnetization and the specific heat are given in Table II. They decrease rapidly with increasing Th content, and the long-range magnetic order vanishes for about 35% Th. For Lu substitution, the suppression of ferromagnetism is even faster: $U_{0.85}Lu_{0.15}RhAl$ is on the verge of the long-range ferromagnetism.

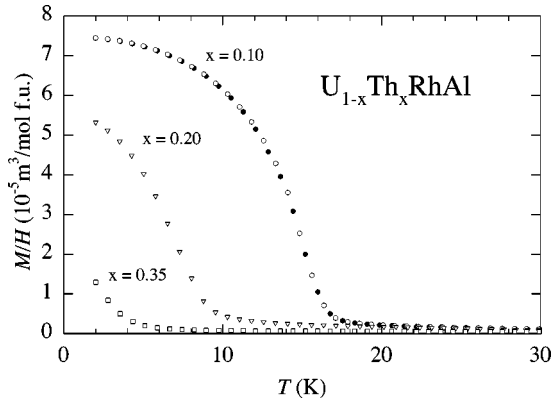


FIG. 3. Temperature dependence of M/H measured as field cooled in 0.01 T for $U_{1-x}Th_xRhAl$ with $x=0.10$, 0.20, and 0.35 (open symbols). For comparison, the zero-field cooled data for $x=0.10$ are also shown (filled circles).

C. Specific heat

The specific heat of the $U_{1-x}Th_xRhAl$ series is represented in Fig. 6. The samples with low substitution exhibit very pronounced anomalies associated with the magnetic phase transition. It turns into a broad bump for 20% of Th, and only an upturn at low T appears for higher Th concentration. The shift of T_C to lower temperatures with increasing thorium content is clearly seen here. We observe a similar trend in the $U_{1-x}Lu_xRhAl$ series.

The specific heat in the studied compounds consists generally of three contributions: the lattice (phonon) specific heat C_{ph} , the electronic part C_{el} , and the magnetic specific heat C_{mag} . In the case of nonmagnetic ThRhAl and LuRhAl, the magnetic part is zero and the analysis is more straightforward. The γ coefficient characterizing the electronic contribution is easily obtained from the C_p/T vs T^2 plot at low temperatures. The fit to our experimental data below 10 K gives $\gamma=4$ mJ K $^{-2}$ mol $^{-1}$ and 3 mJ K $^{-2}$ mol $^{-1}$ for ThRhAl and LuRhAl, respectively.

The total phonon spectrum consists of three acoustic and six optical branches in our case (three atoms in the unit cell).

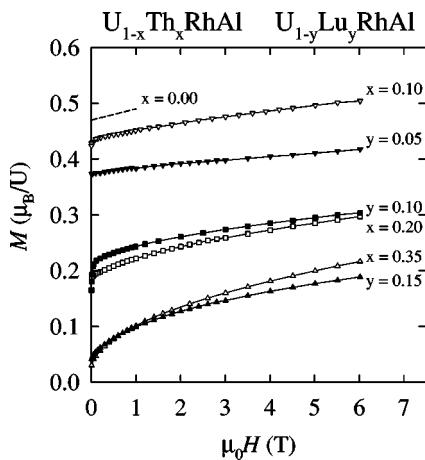


FIG. 4. Magnetization curves for different concentrations in the $U_{1-x}Th_xRhAl$ (open symbols) and $U_{1-y}Lu_yRhAl$ (filled symbols) systems measured at 2 K. The data for URhAl ($x=0.0$) are taken from Ref. 11.

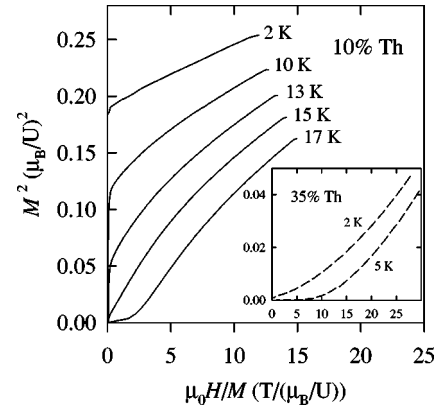


FIG. 5. Arrott plots for $U_{0.90}Th_{0.10}RhAl$ and $U_{0.65}Th_{0.35}RhAl$ (inset) at different temperatures.

We applied the following approximation: the three acoustic branches we described by the Debye model and characterized by one Debye temperature θ_D , the six optical branches we described by the Einstein model and characterized by two different Einstein temperatures θ_E , each describing three branches. Such a model has been used, e.g., in a similar case of UPtAl.¹⁴ A simple model of the phonon spectrum with all nine phonon branches described by a single θ_D value completely fails to describe the experimental data in the whole temperature range. The value of θ_D is determined by the slope of the C_p/T vs T^2 linear dependence at $T \ll \theta_D$. The fit to experimental data below 10 K gives for the three acoustic branches in our model $\theta_D=149$ K and $\theta_D=170$ K for ThRhAl and LuRhAl, respectively. Further fit to our data of ThRhAl, keeping this value of θ_D , gives the Einstein temperatures $\theta_{E1}=175$ K and $\theta_{E2}=442$ K. As LuRhAl is not relevant as a background compound due to its different crystal structure, we did not perform analogous analysis in this case.

To obtain the magnetic specific heat in the magnetically ordered compounds, one has to subtract the phonon and the electronic contributions. As a first approximation, we took the phonon contribution of ThRhAl plus the electronic specific heat characterized by $\gamma=45$ mJ K $^{-2}$ mol f.u. $^{-1}$. Such an approximation gives a good agreement with the measured data of all magnetically ordered compounds between T_C and

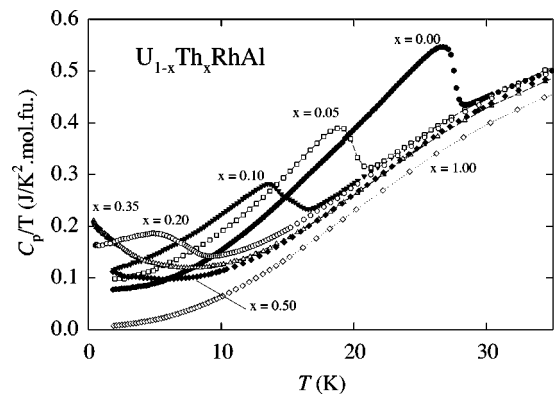


FIG. 6. The C_p/T vs T dependencies for the $U_{1-x}Th_xRhAl$ series.

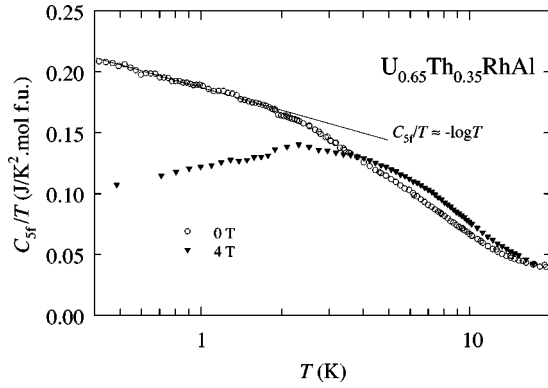


FIG. 7. The C_{5f}/T vs $\log T$ data for $U_{0.65}Th_{0.35}RhAl$; the electronic ($5f$) contribution to the specific heat has been obtained by subtraction of the lattice part from the measured data.

100 K. The corresponding magnetic entropy is given in Table II. These values represent an upper entropy estimate because (i) our analysis of URhAl data below 10 K suggests slightly smaller θ_D value (≈ 135 K) that would lead to a higher phonon contribution and (ii) we take a constant C_{mag}/T value between the lowest measured temperature and 0 K, while in reality one expects a decrease to zero. This upper limit of entropy in URhAl ($0.40 R \ln 2$) is comparable to the entropy in UNiGa,¹⁵ but considerably lower than in UPtAl ($0.71R \ln 2$).¹⁴ The entropy clearly decreases with Th or Lu substitution, even when related to the U concentration instead to the formula unit.

The real γ value can be determined as the $C_p/T(T \rightarrow 0 \text{ K})$ limit from the low-temperature data. These values, given in Table II, increase considerably with dilution by Th or Lu, reaching a moderate heavy-fermion value of $230 \text{ mJ K}^{-2} \text{ mol f.u.}^{-1}$ for 35% of Th. By applying the magnetic field, the high γ values in compounds with high content of Th or Lu ($x > 0.1$) are strongly reduced (e.g., from $\approx 230 \text{ mJ K}^{-2} \text{ mol f.u.}^{-1}$ in 0 T to $\approx 100 \text{ mJ K}^{-2} \text{ mol f.u.}^{-1}$ in 4 T for the 35% Th sample), while the γ value in URhAl remains almost field independent.

The $C_p/T(T)$ dependence for 35% Th exhibits a strong upturn at low T . Taking the same lattice specific heat in $U_{0.65}Th_{0.35}RhAl$ as in ThRhAl and plotting the remaining electronic part C_{5f} divided by T vs $\log T$ (shown in Fig. 7), one can observe a linear dependence between 0.4 K and 2 K. Another linear part with a different slope is seen between 2 K and 10 K. Such logarithmic dependence is often attributed to a non-Fermi-liquid (NFL) behavior.¹⁶ However, the specific heat in the NFL systems follows such dependence usually in a broader temperature range, at least over one decade. The increase between 2 K and 0.4 K is not large in our case. We thus cannot unambiguously characterize this compound as a NFL system.

IV. DISCUSSION

Let us now discuss qualitatively the development of the electronic properties in the studied system. The nonmagnetic ground state and the low γ value of the electronic specific heat in ThRhAl and LuRhAl are consistent with the absence

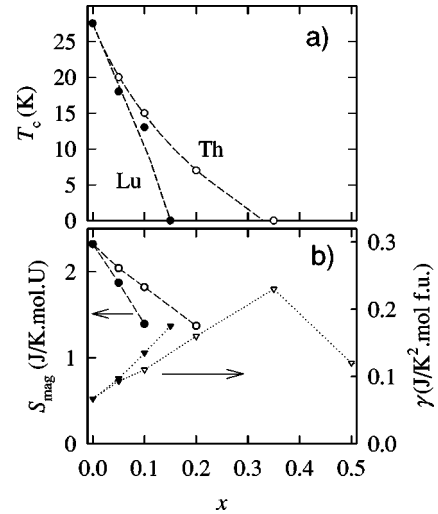


FIG. 8. Concentration dependence of (a) the ordering temperature, (b) the γ coefficient of low-temperature specific heat and the magnetic entropy. The open and filled symbols concern always $U_{1-x}Th_xRhAl$ and $U_{1-x}Lu_xRhAl$ compounds, respectively.

of the $5f$ electronic states near the Fermi energy E_F in ThRhAl (or $4f$ states in LuRhAl). By increasing the uranium content, we observe first an enhancement of the γ value, which can be associated with a formation of a relatively narrow resonance of quasiparticle states at the Fermi level. The γ value reaches a maximum in the concentration region where the long-range ferromagnetic order appears. Further increase of uranium concentration leads to growth of the uranium moments, to a strengthening of the ferromagnetic exchange interactions, and consequently to the increase of the critical temperature, the ordered magnetic moment and the magnetic entropy (see Fig. 8). Considering the $5f$ bonding anisotropy to be the main mechanism responsible for the magnetocrystalline anisotropy² in the studied compounds, we assume the uniaxial magnetic order with the c axis as the easy-magnetization direction. With the onset of the magnetic order, the γ values decrease. Besides the suppression of many-body phenomena related to the onset of magnetism we may think of removing part of the $5f$ states from E_F due to the splitting of spin-up and spin-down subbands. But it is interesting to note that the γ value in the ordered state ($T \rightarrow 0 \text{ K}$) in pure URhAl ($\gamma = 67 \text{ mJ K}^{-2} \text{ mol}^{-1}$) is higher than that in the paramagnetic state ($\gamma = 45 \text{ mJ K}^{-2} \text{ mol}^{-1}$ estimated from comparison to ThRhAl as described in Sec. III C.), which contradicts the latter possibility.

The comparison of (U,Th)RhAl with (U,Lu)RhAl excludes explanation of the suppression of magnetism as due to the change of the conduction electron concentration (Fermi-level tuning). Both tetravalent Th and trivalent Lu lead to a fast suppression of magnetism (uranium is usually assumed to be trivalent in this type of compounds).

When putting (U,Th)RhAl and (U,Lu)RhAl to the context of several other isostructural systems mentioned in the Introduction, we deduce that they differ from the local-moment system (U,Th)CoSn by much faster suppression of ferromagnetism. For example, $(U_{0.65}Th_{0.35})RhAl$ resembles very much, including the pronounced low- T upturn in C/T vs T ,

($U_{0.20}Th_{0.80}$)CoSn. For the Lu dilution, the suppression of ferromagnetism is even faster, presumably due to a size effect. In the systems with Th, the dilution of the U sublattice as the destructive mechanism for the $5f$ magnetism is partly compensated by an increasing volume; which normally leads to the stabilization of the $5f$ moments. For the substitution with smaller Lu atoms, the volume increase is absent.

The dilution can be conceived either as the destruction of well-defined $5f$ band states first by the loss of coherence (in early stage of dilution), then as decay into individual impurity states (for higher dilution). In a qualitatively similar way we could characterize the development for the U magnetism with not so pronounced features of band magnetism, for which hybridization-induced exchange interaction picture is more appropriate. On the other hand, (U,Th)RhAl differs from the systems mentioned in the Introduction as weak itinerant magnets. The difference is that the concentration with undoubtedly nonmagnetic ground state (15% Lu, 35% Th) exhibit still the paramagnetic susceptibility of the Curie-Weiss type and not the Pauli type.

V. CONCLUSIONS

The substitution of the U atoms by Th or Lu in URhAl leads to a suppression of the ferromagnetic order. The mag-

netization and specific-heat data reveal a decrease of the ordering temperature, the spontaneous magnetization, the magnetic entropy, and the paramagnetic effective moment with the Th or Lu substitution. The suppression of ferromagnetism is faster for the Lu substitution. The compounds with 35% Th and 15% Lu are on the verge of the long-range ferromagnetism, and a maximum of the electronic specific heat appears in these critical concentration regions. We demonstrated that the substitution of the U sublattice is a convenient tool to study the degree of the delocalization of the $5f$ states. URhAl is an intermediate case between the weak itinerant magnets and $5f$ local-moment systems.

ACKNOWLEDGMENTS

This work is a part of the research Program No. MSM113200002 that is financed by the Ministry of Education of the Czech Republic. P.J. acknowledges the European Commission for support given in the frame of the program "Training and Mobility of Researchers." This work was also supported by the Grant Agency of the Czech Republic under Grant No. 202/04/1103.

*Electronic address: javor@mag.mff.cuni.cz

¹V. Sechovský and L. Havela, in *Ferromagnetic Materials—A Handbook on the Properties of Magnetically Ordered Substances*, edited by E.P. Wohlfarth and K.H.J. Buschow (North-Holland, Amsterdam, 1988), Vol. 4, pp. 309–491.

²V. Sechovský and L. Havela, in *Handbook of Magnetic Materials*, edited by K.H.J. Buschow (Elsevier Science B.V., Amsterdam, 1998), Vol. 1, pp. 1–289.

³F.U. Hillebrecht, H.J. Trodahl, V. Sechovský, and B.T. Thole, *Z. Phys. B: Condens. Matter* **77**, 373 (1989).

⁴H. Amitsuka, K. Kuwahara, M. Yokoyama, K. Tenya, T. Sakakibara, M. Mihlik, and A. Menovsky, *Physica B* **281-282**, 326 (2000).

⁵V. Sechovský, L. Havela, G. Hilscher, N. Pillmayr, A.V. Andreev, P.A. Veenhuizen, and F.R. de Boer, *J. Appl. Phys.* **63**, 3070 (1988).

⁶D.D. Koelling, B.D. Dunlap, and G.W. Crabtree, *Phys. Rev. B* **31**, 4966 (1985).

⁷A.V. Andreev, M. Kosaka, Y. Uwatoko, and V. Sechovský, *J. Alloys Compd.* **45**, 309 (2000).

⁸L. Havela and V. Sechovský, in *Electron Correlations and Mate-*

rials Properties, edited by A. Gonis, N. Kioussis, and M. Ciftan (Kluwer Academic/Plenum, Dordrecht, New York, 1999), pp. 169–178.

⁹L. Havela, V. Sechovský, F.R. de Boer, E. Brück, P.A. Veenhuizen, J.B. Bouwer, and K.H.J. Buschow, *J. Magn. Magn. Mater.* **76-77**, 89 (1988).

¹⁰E. Brück, F.R. de Boer, P. Nozar, V. Sechovský, L. Havela, K.H.J. Buschow, and A.V. Andreev, *Physica B* **163**, 379 (1990).

¹¹P.A. Veenhuizen, F.R. de Boer, A.A. Menovsky, V. Sechovský, and L. Havela, *J. Phys. C* **8**, 485 (1988).

¹²A.V. Andreev, J. Kamarád, F. Honda, G. Oomi, V. Sechovský, and Y. Shiokawa, *J. Alloys Compd.* **314**, 51 (2001).

¹³T.D. Cuong, Z. Arnold, J. Kamarád, A.V. Andreev, L. Havela, and V. Sechovský, *J. Magn. Magn. Mater.* **157-158**, 694 (1996).

¹⁴A.V. Andreev, M. Diviš, P. Javorský, K. Prokeš, V. Sechovský, J. Kuneš, and Y. Shiokawa, *Phys. Rev. B* **64**, 144408 (2001).

¹⁵A.V. Andreev, V. Sechovský, P. Javorský, M.I. Bartashevich, T. Goto, Y. Homma, Y. Shiokawa, and D. Rafaja, *J. Alloys Compd.* **319**, 29 (2001).

¹⁶G.R. Stewart, *Rev. Mod. Phys.* **73**, 797 (2001), and references therein.